ACCELERATED TESTING FOR LONG-TERM DURABILITY OF VARIOUS FRP LAMINATES FOR MARINE USE

Masayuki Nakada and Yasushi Miyano
Materials System Research Laboratory, Kanazawa Institute of Technology

Keywords: *FRP, Strength, Fatigue, Accelerated Testing, Durability, Marine*

Abstract

The prediction of long-term fatigue life of various FRP laminates combined with resins, fibers and fabrics for marine use under temperature and water environments were performed by our developed accelerated testing methodology based on the time-temperature superposition principle (TTSP). The five kinds of FRP laminates were prepared under three water absorption conditions of Dry, Wet and Wet+Dry after molding. The three-point bending constant strain rate (CSR) and fatigue tests for these FRP laminates at three conditions of water absorption were carried out at various temperatures and loading rates. As results, the mater curves of fatigue strength as well as CSR strength for these FRP laminates at three water absorption conditions are constructed by using the test data based on TTSP. It is possible to predict the long-term fatigue life for these FRP laminates under an arbitrary temperature and water absorption conditions by using the master curves. The characteristics of time, temperature and water absorption dependencies of flexural CSR and fatigue strengths of these FRP laminates are clarified.

1 Introduction

Recently carbon fiber reinforced plastics (CFRP) has been used for the primary structures of airplanes, ships, spacecrafts and others, in which the high reliability should be kept during the long-term operation. Therefore, it is strongly expected that the accelerated testing methodology for the long-term life prediction of composite structures exposed under the actual environments of temperature, water, and others is established.

The mechanical behavior of polymer resins exhibits time and temperature dependence, called viscoelastic behavior, not only above the glass transition temperature T_g but also below T_g [1-8]. Furthermore, the viscoelastic behavior of polymer resins also depends on the water absorption [9-12]. Thus, it can be presumed that the mechanical behavior of polymer composites significantly depends on the water absorption as well as time and temperature.

This paper is concerned with the prediction of long-term fatigue life of five kinds of FRP laminates for marine use under temperature and water environments. These FRP laminates were prepared under three water absorption conditions of Dry, Wet and Wet+Dry after molding. The three-point bending constant strain rate (CSR) tests for five kinds of FRP laminates at three conditions of water absorption were carried out at various temperatures and strain rates. Furthermore, the three-point bending fatigue tests for these specimens were carried out at various temperatures and frequencies. The characteristics of time, temperature, and water absorption dependencies of flexural fatigue strength as well as flexural CSR strength for these FRP laminates are discussed by our developed accelerated testing methodology based on the time-temperature superposition principle (TTSP) shown in Fig.1.

Our accelerated testing methodology which rests on the three hypotheses, (A) same time-temperature superposition principle for all strengths, (B) linear cumulative damage law for monotonic loading, and (C) linear dependence of fatigue strength upon stress ratio. When these hypotheses are met, the fatigue strength under an arbitrary combination of frequency, stress ratio, and temperature can be determined based on the following test results: (a) master curve of strength under constant strain-rate (CSR) loading and (b) master curve of fatigue strength for zero stress ratio. The master curve of CSR strength is constructed

from the test results at various constant strain-rates and temperatures. On the other hand, the master curve of fatigue strength at zero stress ratio can be constructed from the test results at single frequency for various temperatures based on the hypothesis (A). The details of accelerated testing methodology can be obtained from our published papers [13-18].

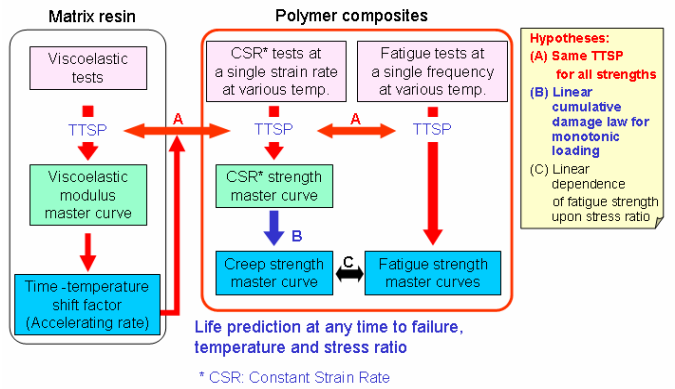

Fig.1 Accelerated testing methodology for polymer composites

2 Experimental Procedures

2.1 Preparation of specimens

The base material of five kinds of FRP laminates employed in this study was plain fabric CFRP laminates T300 carbon fibers/vinylester (T300/VE). The first selection of FRP laminate to T300/VE was the combinations of different fabrics, that is flat yarn plain fabric T700 carbon fibers/vinylester (T700/VE-F) and multi-axial knitted T700 carbon fibers/vinylester (T700/VE-K) for marine use and the second selection of FRP laminates to T300/VE was the combinations with different fibers and matrix resin, that is plain fabric T300 carbon fibers/epoxy (T300/EP) and plain fabric E glass fibers/vinylester (E-glass/VE) shown in Fig.2. These FRP laminates were formed by resin transfer molding (RTM) except T300/EP which was formed by conventional hand lay up. The thickness of the laminates was approximately 2mm.

	T300/VE	T700/VE・F	T700/VE・K	T300/EP	Eglass/VE
Weave	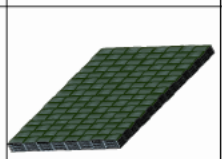 Plain woven : Normal yarn (fiber bundle 2mm)	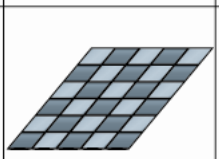 Plain woven : Flat yarn (fiber bundle 10mm)	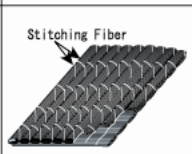 Knitted fabric	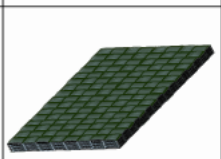 Plain woven : Normal yarn (fiber bundle 2mm)	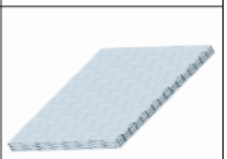 Plain woven : Normal yarn (fiber bundle 2mm)
Fiber	T300-3K-50B	T700SC-12K-50C		T300-3K-50B	WL230-104BS6
Matrix resin	DERAKANE MOMENTUM:100 Permek N:0.8 Cobalt naphthenate:0.06			Epikote 828:100 MHAC-P:103.6 2E4MZ:1	DERAKANE MOMENTUM:100 Permek N:0.8 Cobalt naphthenate:0.06
Number of layers	8	9	4	9	10
Volume fraction	49%	53%	52%	52%	33%
Forming	RTM (Resin Transfer Molding)	RTM (Resin Transfer Molding)	VARTM (Vacuum Assisted RTM)	Hand lay up method	VARTM (Vacuum Assisted RTM)
Cure schedule	25°C × 48h 150°C × 2h	25°C × 48h 150°C × 2h	25°C × 48h 150°C × 2h	70°C × 12h 150°C × 4h 190°C × 2h	25°C × 48h 150°C × 2h

Fig.2 Constitution of five kinds of FRP laminates combined with different resins and fibers

These FRP laminates were prepared under three water absorption conditions of Dry, Wet and Wet+Dry after molding. Dry specimens by holding the cured specimens at 150°C for 2 hours in air, Wet specimens by soaking Dry specimens in hot water of 95°C for 120 hours and Wet+Dry specimens by

dehydrating the Wet specimens at 150°C for 2 hours in air were respectively prepared as shown on Table I. Figure 3 shows water content versus soaking time at 95°C and the soaking condition of 95°C and 120 hours was determined to Wet specimens. Figure 4 shows water content in resin and FRP for Wet and Wet+Dry specimens. The water absorption of all FRP laminates increases with Wet condition of hot water of 95°C for 120 hours. The water absorption of neat vinylester resin and its CFRP laminates returns to 0% with Wet+Dry condition by re-drying and that of T300/EP and E-glass/VE does not return to 0%.

Table I Conditions for Dry, Wet, and Wet+Dry specimens

Specimen	In air	In water	In air
Dry	As cured		
Wet	As cured	+ 95°C x 120h	
Wet+Dry	As cured	+ 95°C x 120h	+ 150°C x 2h

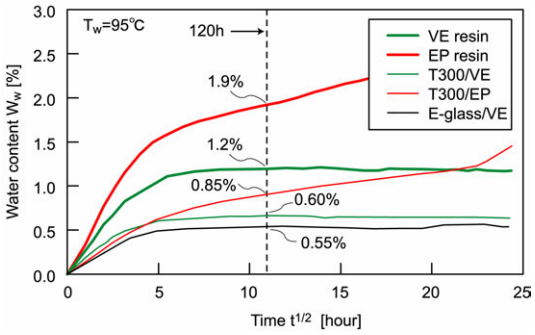

Fig.3 Water content versus soaking time

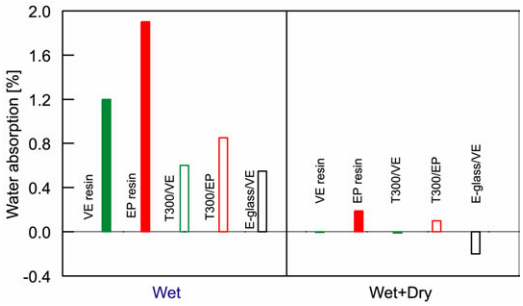

Fig.4 Water content in resin and FRP for Wet and Wet+Dry conditions

2.2 Experimental procedures

Figure 5 shows the configuration of three-point bending test and Table II shows the test conditions. To evaluate the viscoelastic behavior of vinylester (VE) and epoxy (EP) as matrix neat resin, the three-point bending creep tests for the neat vinylester and epoxy resins prepared at Dry, Wet and Wet+Dry conditions were carried out under various temperatures using an creep testing machine with temperature chamber. The creep compliance D_c was calculated from the deflection δ at the center of specimen using the following equation:

$$D_c = \frac{4bh^3\delta}{P_0 L^3} \quad (1)$$

where P_0 is the applied constant load (58.8N), L is the span (50mm), and b and h are the width (25mm) and the thickness (3.0mm) of specimen, respectively.

The three-point bending CSR tests for five kinds of FRP laminates at Dry, Wet and Wet+Dry conditions were carried out at various temperatures and strain rates. The span is L=80mm, and the width and thickness are b=15mm and h=2.0mm, respectively. The CSR tests were conducted at three loading-rates V=0.02, 2, 200 mm/min and various constant temperatures T using an universal testing machine with temperature chamber. The flexural CSR strength σ_s is calculated from the maximum load P_s by

$$\sigma_s = \frac{3P_s L}{2bh^2}. \quad (2)$$

Furthermore, the three-point bending fatigue tests for these specimens were carried out at various constant temperatures T and two loading frequencies f=2Hz and 0.02Hz using an electro-hydraulic servo testing machine with temperature chamber. The stress ratio R (= minimum stress/maximum stress) was 0.05. The length, width, thickness of specimen, and span are the same to those for the flexural CSR tests. The flexural fatigue strength σ_f is defined by maximum applied load P_{max} for the number of cycles to failure N_f.

$$\sigma_f = \frac{3P_{max} L}{2bh^2}. \quad (3)$$

In order to prevent the dryness of specimens at Wet condition during creep, CSR, and fatigue tests, the specimens were wrapped by a vinyl bag with including distilled water in the bag.

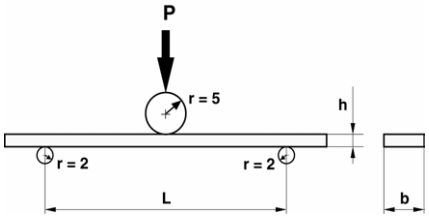

Fig.5 Configuration of three point bending test

Table II Test conditions

Loading type	Deflection rate V [mm/min]	Frequency f [Hz]	Stress ratio R [$\sigma_{min}/\sigma_{max}$]	Temperature T [°C]
Creep for neat resin	—	—	—	25 ~ 150
CSR for FRP	0.02*, 2, 200*	—	—	25 ~ 160
Fatigue for FRP	—	0.02*, 2	0.05	25 ~ 140

* : Test conditions for confirming of applicability of TTSP

3 Results and Discussion

3.1 Creep compliance

The left sides of upper graphs in Fig.6 show the creep compliance D_c versus testing time t at various temperatures T for Dry, Wet and Wet+Dry specimens of VE and EP resin. The master curves of D_c versus the reduced time t' were constructed by shifting D_c at various constant temperatures along the log scale of t and the log scale of D_c. Since the smooth master curve of D_c for each specimen can be obtained as shown in the right sides of each graph, the time-temperature superposition principle (TTSP) is applicable for each D_c. From these master curves, it is cleared that D_c increases with water absorption and returns perfectly to that of Dry specimen by re-drying after water absorption.

The horizontal time-temperature shift factor $a_{T_0}(T)$ and the vertical temperature shift factor $b_{T_0}(T)$ at a reference temperature T_0 plotted in lower graphs in Fig.6 are respectively defined by

$$\log a_{T_0}(T) = \log t - \log t' \tag{4}$$

$$\log b_{T_0}(T) = \log D_c(t,T) - \log D_c(t',T_0) \tag{5}$$

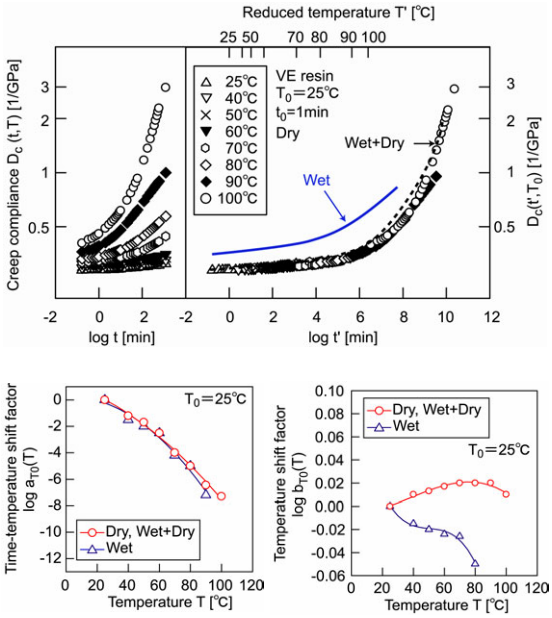

Fig.6-1 Master curve of creep compliance for neat vinylester resin and shift factors

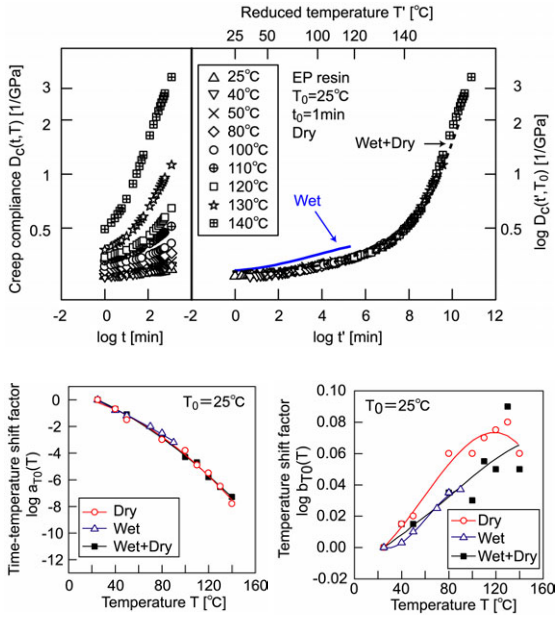

Fig.6-2 Master curve of creep compliance for neat epoxy resin and shift factors

3.2 Flexural CSR strength

The left side of each graph in Fig.7 shows the flexural CSR strength σ_s versus time to failure t_s at various temperatures T for Dry, Wet and Wet+Dry specimens of five kinds of FRP laminates, where t_s is the time period from initial loading to maximum load during testing. The master curves of σ_s versus the reduced time to failure t_s' were constructed by shifting σ_s at various constant temperatures along

the log scale of t_s and the log scale of σ_s using the same time-temperature shift factors and a half of the temperature shift factors for D_c of matrix resin shown in Fig.6. The reason why the shift amount to the log scale of σ_s is a half of that to the log scale of D_c is mentioned after. Since the smooth master curve of σ_s for each specimen can be obtained as shown in the right side of each graph, the TTSP for D_c of matrix resin is also applicable for the σ_s of corresponding FRP laminates. It is cleared from Fig.7 that the σ_s for all five FRP laminates strongly decreases with increasing time and temperature and that these σ_s decreases with water absorption and returns to that of Dry specimens by re-drying after water absorption except that of GFRP laminates (E-glass/VE). The σ_s of Wet+Dry specimens of E-glass/VE does not return to that of Dry specimens.

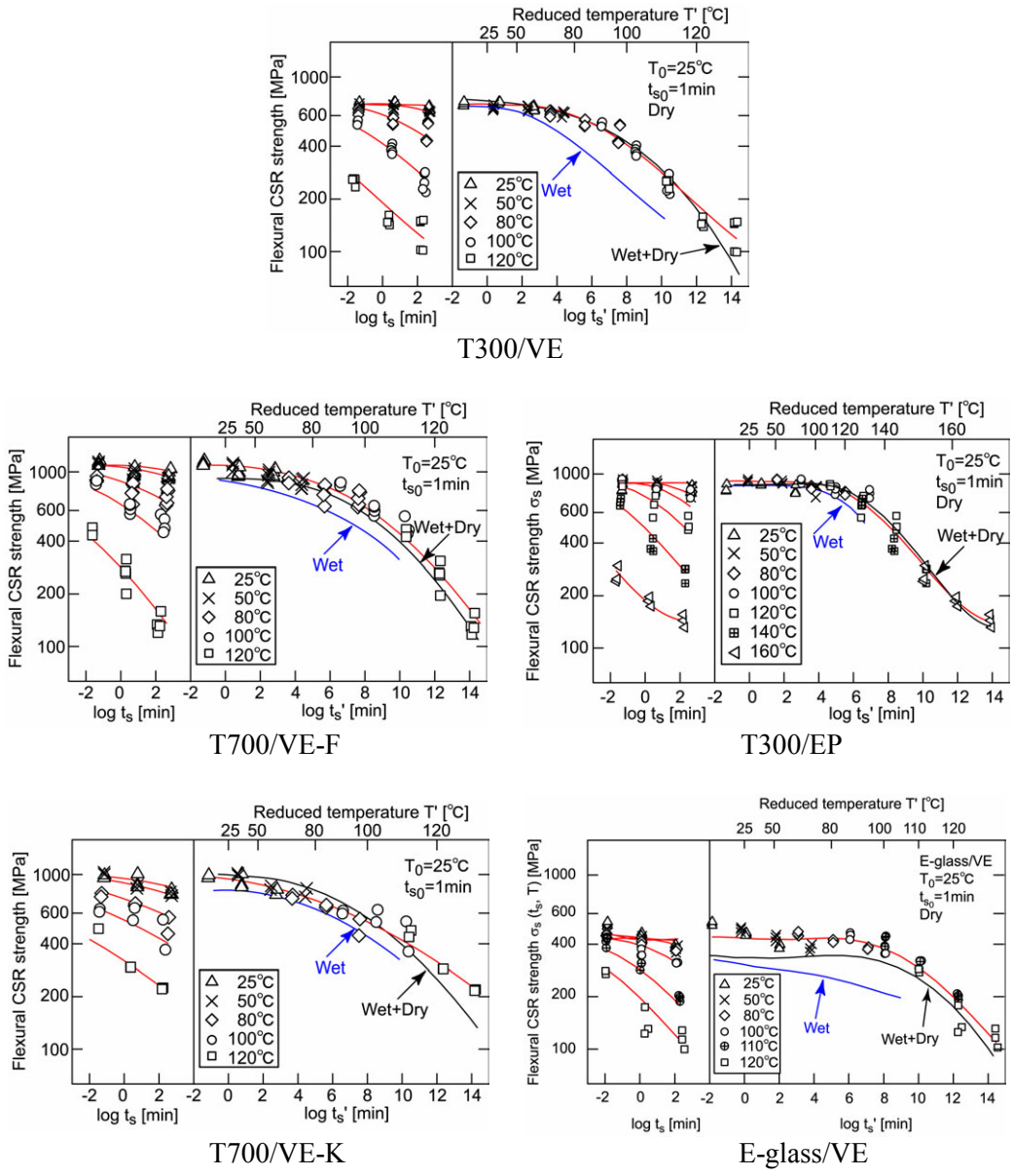

Fig.7 Master curves of flexural CSR strength at Dry, Wet and Wet+Dry conditions

Figure 8 shows the flexural CSR strength versus the creep compliance of matrix resin for the same conditions of time, temperature and water absorption for five FRP laminates. The degradation of flexural CSR strength for all CFRP laminates except GFRP laminates (E-glass/VE) is uniquely

determined by the creep compliance of matrix resin. Therefore, the degradation rate of flexural CSR strength of these CFRP laminates is determined only by increasing of time, temperature and water absorption and is independent upon fiber constitutions which are the type, volume fraction and weaves. The slope is approximately 0.5 shown in each graph of this figure. This indicates that the trigger of failure is the microbuckling of carbon fibers in the compression side of specimen shown by the following equation based on Dow's theory [19]:

$$\log \sigma_s = \log K' - \frac{1}{2} \log D_c \qquad (6)$$

where σ_s is the CSR strength of CFRP laminates, K is the material constant and D_c is the creep compliance of matrix resin. Actually, the fracture appearance indicates that the fracture mode for these CFRP laminates is the compressive fracture of warp carbon fibers in the compression side of specimen for all condition tested as shown in Fig.9. Therefore, this is the reason why the vertical shift amount for σ_s is a half of that for D_c as mentioned above. The fracture mode for T300/EP laminates and E-glass/VE is the tensile fracture in the tension side of specimen at T=25°C. However the fracture mode at high temperatures is the compressive fracture in the compression side of specimen same to that for T300/VE laminates.

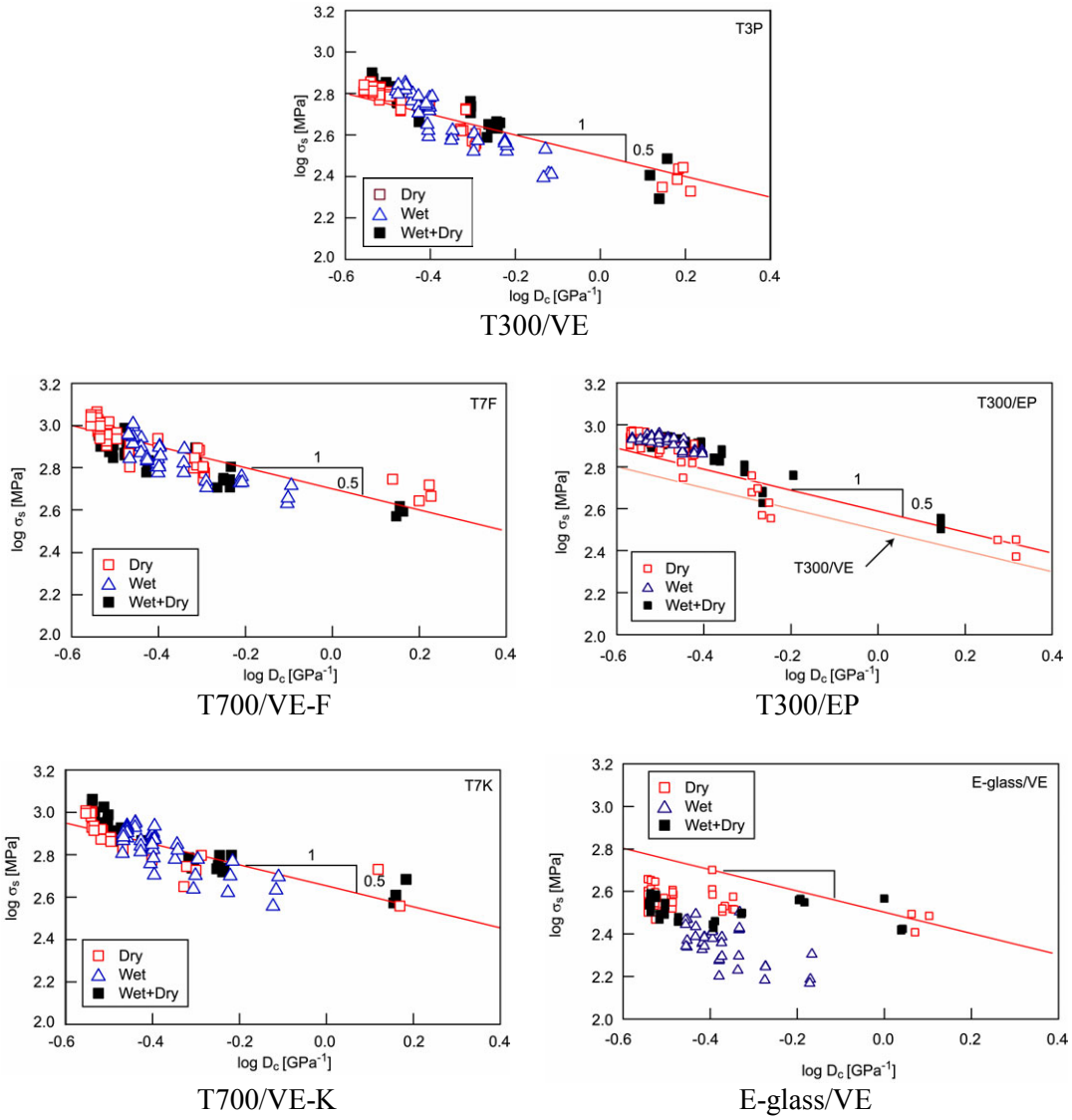

Fig.8 Flexural CSR strength versus creep compliance of matrix resin at Dry, Wet and Wet+Dry conditions

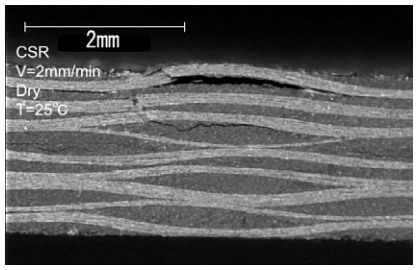

T300/VE

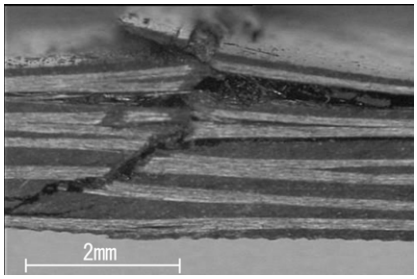

T700/VE-F

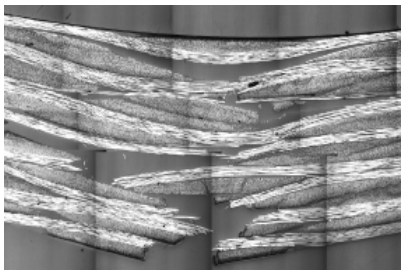

T300/EP

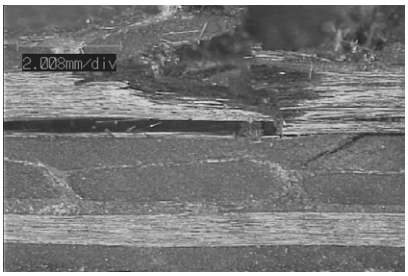

T700/VE-K

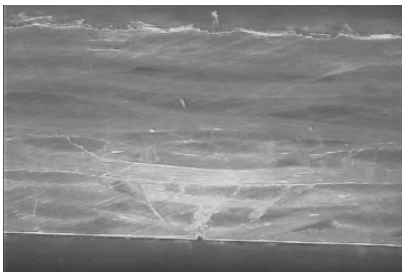

E-glass/VE

Fig.9 Fracture appearances of specimens after flexural CSR test at 25 °C at Dry condition

3.3 Flexural fatigue strength

To construct the master curve of flexural fatigue strength σ_f, we need the reduced frequency f' in addition to the reduced time to failure t_f', each defined by

$$f' = f \cdot a_{T_0}(T) \quad , \qquad t_f' = \frac{t_f}{a_{T_0}(T)} = \frac{N_f}{f'} \tag{7}$$

where N_f is the number of cycles to failure.

The σ_f versus N_f at frequency f=2Hz at various temperatures were measured for Dry, Wet and Wet+Dry specimens of five kinds of FRP laminates. For examples, the σ_f versus N_f curves at various temperatures for Dry specimen are shown in Fig.10. By converting f and N_f into f' and t_f' using Eq.7, the time-temperature shift factors $a_{To}(T)$ and temperature shift factors $b_{To}(T)$ of the creep compliance of matrix resin for each specimen shown in Fig.6, the σ_f versus t_f' for each f' were constructed for Dry, Wet and Wet+Dry specimens of five kinds of FRP laminates shown in Figs.11-1 and 11-2. The curves consisted by solid circles in these graphs show the master curves of CSR strengths which can be considered as the fatigue strength at stress ratio R=0 and N_f=1/2. Each curve consisted by hollow circles in these graphs shows the curve of fatigue strength σ_f versus reduced time to failure t_f' at each reduced frequency f' to diverge from the master curve of CSR strength.

In order to confirm the applicability of TTSP for fatigue strength, we predicted the σ_f-N_f curves at f=0.02Hz and compared them with the test results. The predicted σ_f from fatigue master curves for all FRP laminates agree well with experimental ones, therefore, the TTSP for the creep compliance of matrix resin also holds for fatigue strength of the corresponding FRP laminates.

It is cleared from Figs.11-1 and 11-2 that the σ_f of all five FRP laminates strongly decreases with time to failure, temperature and water absorption

and that the σ_f of four kinds of FRP laminates except GFRP laminates (E-glass/VE) decreases scarcely with N_f although that of E-glass/VE decreases strongly with N_f And the degradation rate to time and temperature for the fatigue strength σ_f of these CFRP laminates is very similar to that for CSR strength. The σ_f of all FRP laminates also decreases with water absorption and that returns to that of Dry specimens by re-drying after water absorption except that of T300/EP in the range of long time and that of E-glass/VE in all range of time employed. The σ_f of Wet+Dry specimens of T300/EP and E-glass/VE does not return to that of Dry specimens and shows irreversible behavior.

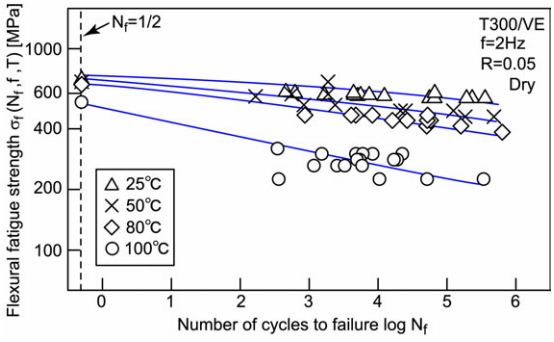

T300/VE

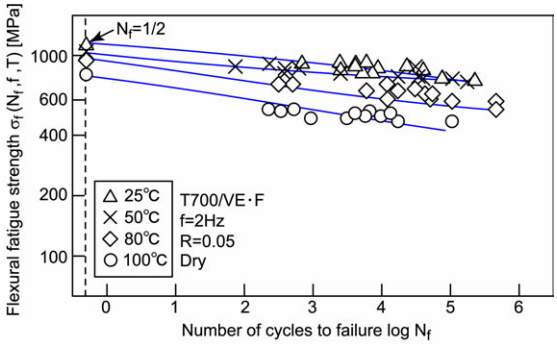

T700/VE-F

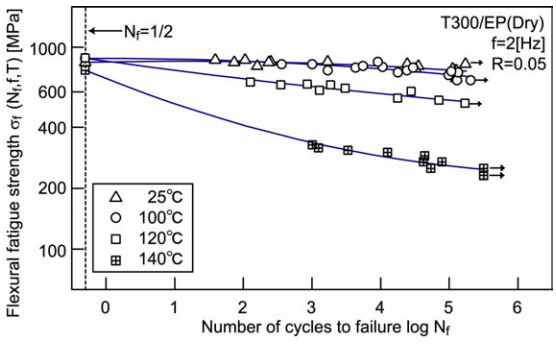

T300/EP

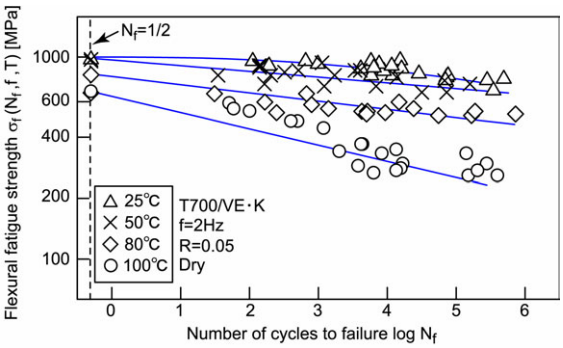

T700/VE-K

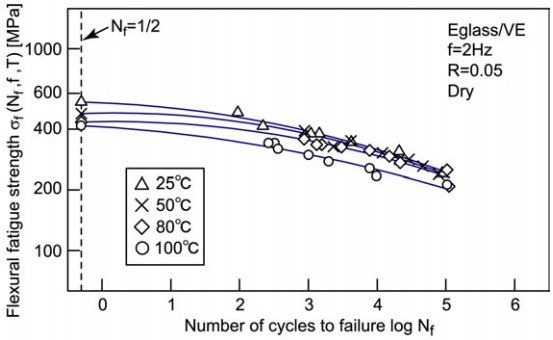

E-glass/VE

Fig.10 σ_f versus N_f curves at frequency 2Hz for Dry specimen

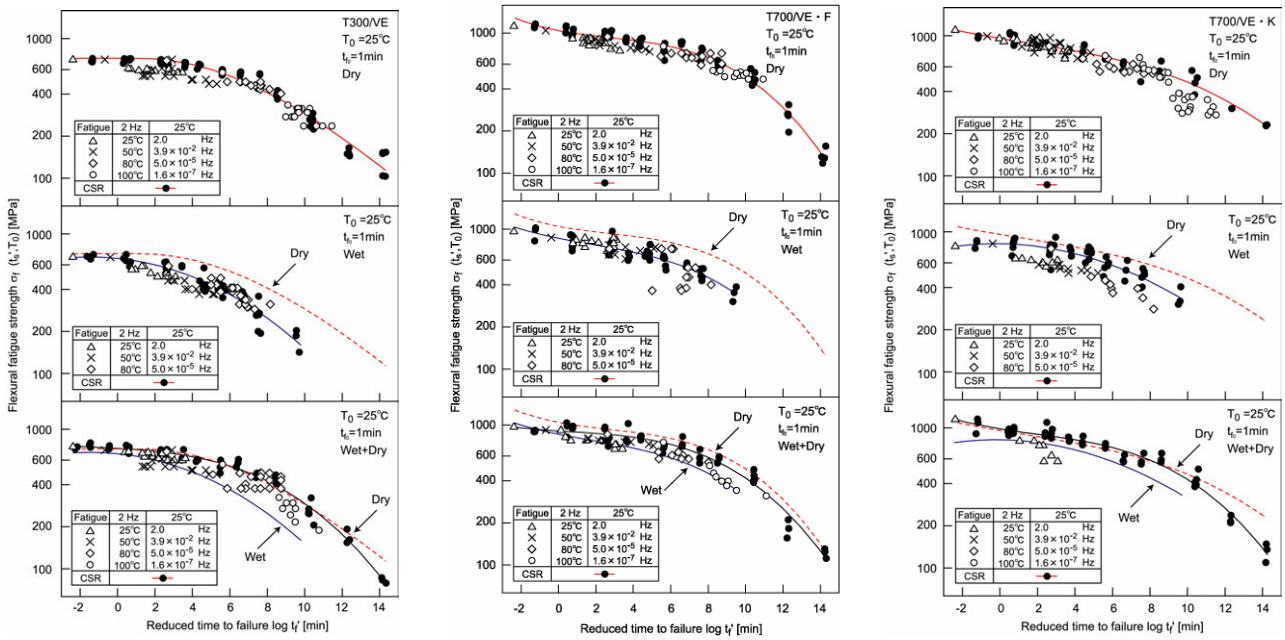

Fig.11-1 Master curves of flexural fatigue strength for T300/VE, T700/VE-F and T700/VE-K

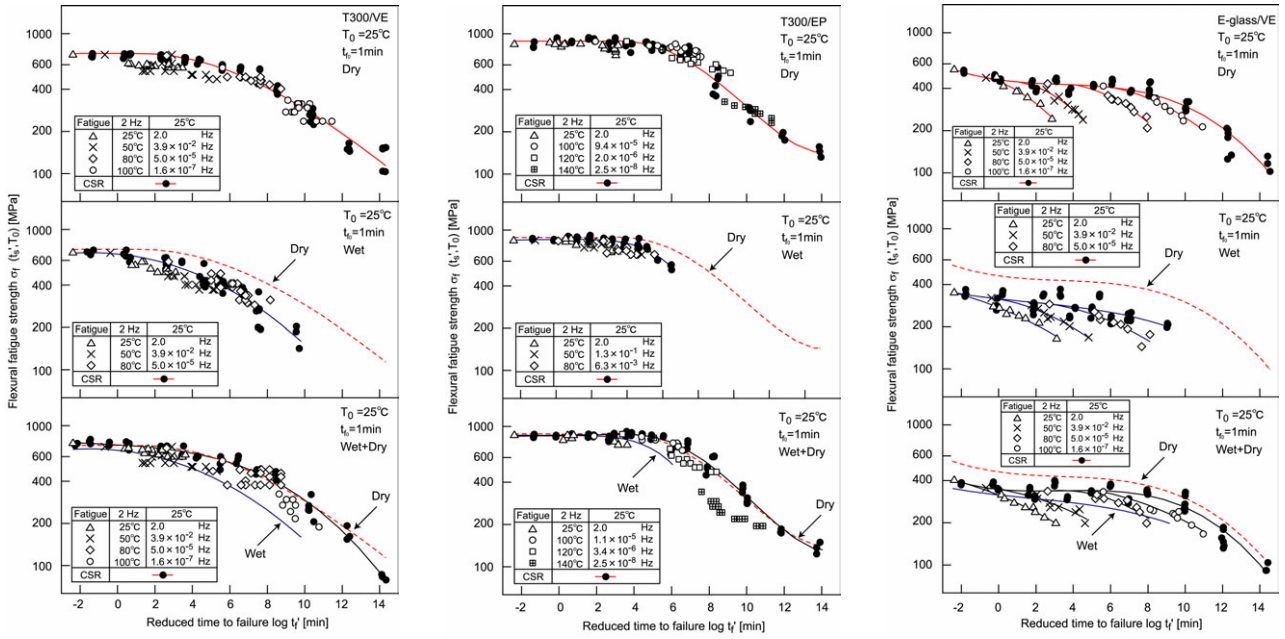

Fig.11-2 Master curves of flexural fatigue strength for T300/VE, T300/EP and E-glass/VE

4 Conclusion

The prediction of long-term fatigue life of five kinds of FRP laminates combined with matrix resin, fiber and fabric for marine use under temperature and water environments were performed by our developed accelerated testing methodology based on the time-temperature superposition principle (TTSP). The three-point bending CSR and fatigue tests for five kinds of FRP laminates at three conditions of water absorption were carried out at various temperatures and loading rates.

As results, the flexural fatigue strength of three kinds of CFRP laminates with vinylester resin as matrix strongly depends on water absorption as well as time and temperature, however scarcely depends on the number of cycles to failure. The mater curves of fatigue strength for these CFRP laminates are constructed by using the test data based on TTSP. The fatigue strength of these CFRP laminates decreases with water absorption and that returns to the initial fatigue strength by re-drying after water absorption. It is possible to predict the long term fatigue life for these CFRP laminates under an arbitrary temperature and water absorption conditions by using the master curves. Furthermore, it is clear that the degradation rate of fatigue strength of these CFRP laminates is determined only by increasing of time, temperature and water absorption and is independent upon fiber constitutions which are the type, volume fraction and weaves.

On the other hand, CFRP laminates with epoxy resin as matrix and GFRP laminates with vinylester resin as matrix chemically change by the process of water absorption and re-drying and the flexural fatigue strength of these FRP laminates decrease with this process.

Acknowledgements

The authors thank the Office of Naval Research for supporting this work through an ONR award (N000140110949) with Dr. Yapa Rajapakse as the program manager of solid mechanics. The authors thank Professor Richard Christensen at Stanford University as the consultant of this project and Toray Industries, Inc. as the supplier of CFRP laminates. All of experimental data were measured by the staffs and graduate students of author's laboratory, Kanazawa Institute of Technology. The authors thank these staffs and graduate students, Dr. Naoyuki Sekine, Dr. Junji Noda, Ms. Jun Ichimura, Mr. Eiji Hayakawa and Mr. Takahito Uozu.

References

1. Aboudi, J. and Cederbaum, G., Composite Structures, 12: 243-256 (1989).
2. Sullivan, J. L., Composite Science and Technology, 39: 207-232 (1990).
3. Gates, T., Experimental Mechanics, 68-73 (1992).
4. Miyano, Y., Kanemitsu, M., Kunio, T. and Kuhn, H., J. Composite Materials, 20: 520-538 (1986).
5. Miyano, Y., McMurray, M. K., Enyama, J., and Nakada, M., J. Composite Materials, 28: 1250-1260 (1994).
6. Miyano, Y., K. McMurray, M., Kitade, N., Nakada, M. and Mohri, M., Advanced Composite Materials, 4: 87-99 (1994).
7. Miyano, Y., Nakada, M., and McMurray, M. K., J. Composite Materials, 29: 1808-1822 (1995).
8. Miyano, Y., Nakada, M., McMurray, M. K. and Muki, R., J. Composite Materials, 31: 619-638 (1997).
9. Shen, C. H and Springer, G. S., J. Composite Materials, 10: 2-20 (1976).
10. Kibler, K. G., AGRD Conference Proceedings, 8-1, (1980).
11. Neumann, S. and Marom, G., Polymer Composites, 6: 9-12 (1985).
12. Selzer, R., and Friedrich, K., Composites Part A, 28A: 595-604 (1997).
13. Miyano, Y., Nakada, M., Kudo, H. and Muki, R., Prediction of Tensile Fatigue Life under Temperature Environment for Unidirectional CFRP, Advanced Composite Materials, 8 (1999) 235-246.
14. Miyano, Y., Nakada, M. and Muki, R., Applicability of Fatigue Life Prediction Method to Polymer Composites, Mechanics of Time-Dependent Materials, 3 (1999) 141-157.
15. Miyano, Y., Nakada, M. and Muki, R., Prediction of Fatigue Life of a Conical Shaped Joint System for Fiber Reinforced Plastics under Arbitrary Frequency, Load Ratio and Temperature, Mechanics of Time-Dependent Materials, 1 (1997) 143-159.
16. Sihn, S., Miyano, Y., Nakada, M., and Tsai, S. W., Time- and Temperature-Dependent Failures of a Metal-to-Composites Bonded Joint with PMMA Adhesive Material, Journal of Composite Materials, 37 (2003) 35-54.
17. Miyano, Y., Nakada, M., and Sekine, N., Accelerated testing for long-term durability of GFRP laminates for marine use, Composites Part B, 35 (2004) 497-502.
18. Miyano, Y., Nakada, M., and Sekine, N., Accelerated Testing for Long-term Durability of FRP Laminates for Marine Use, Journal of Composite Materials, 39 (2005) 5-20.
19. Dow, N. F., Gruntfest, I. J., Space Sciences Laboratory, Structures and Dynamics Operation, T.I.S.R60SD389 (1960).